

## MEDIUM AND LARGE-SCALE VARIATIONS OF DYNAMO-INDUCED ELECTRIC FIELDS FROM AE ION DRIFT MEASUREMENTS

W. R. Coley and J. P. McClure  
Center for Space Sciences, Physics Program  
The University of Texas at Dallas  
Richardson, Texas 75083

Current models of the low latitude electric field are largely based on data from incoherent scatter radars. We are extending these observations through the addition of the rather extensive high quality electric field measurements from the Ion Drift Meter (IDM) aboard the Atmosphere Explorer (AE) spacecraft. We present here some preliminary results obtained from the Unified Abstract files of satellite AE-E. This satellite was active from the end of 1975 through June 1981 in various elliptical and circular orbits having an inclination near  $20^\circ$ . The resulting data can be examined for the variation of ion drift with latitude, longitude, season, solar cycle, altitude, and magnetic activity. The results presented here will deal primarily with latitudinal variations of the drift features.

Figure 1 shows data from a single AE-E orbit. Of particular interest is the upward ion drift enhancement at 2:38 UT. This corresponds to 18:30 solar local time (SLT). This enhancement of the upward drift after sunset prior to reversal is a classic pattern that is often seen both by ground-based radar and satellite. However, on many occasions this prereversal enhancement (PRE) is absent. In order to investigate the reasons for these and other variations of the observed drift features it is of course necessary to deal with large quantities of data.

Figures 2a and 2b show the type of data presentation used in this study. Figure 2a is a "mass plot" of vertical drift data from AE-E obtained from the 15-second average values of the Unified Abstract files. All vertical drifts in the file between  $-20^\circ$  and  $20^\circ$  dip latitude (DLAT) for the August-September 1978 time period are plotted versus SLT. In all there are some 6987 points. Figure 2b shows the same data averaged into 30-minute bins. The dotted line represents the 24-hr average vertical drift. For comparison, Figure 3 shows some incoherent scatter radar results from Jicamarca for the July-August 1968-1971 time period (Fejer et al., 1979). In both cases we see the same general features: downward flow at night reversing at 0600 SLT, a daytime peak followed by a decline to a prereversal enhancement between 19 and 20 SLT, and a reversal to downward flow at night.

Figures 4a and 4b cover May-July 1979 from  $-20^\circ$  to  $20^\circ$  DLAT. The satellite was in a near-circular orbit during this period within altitudes of 450-475 km. There are some 17,000 points plotted on Figure 4a, most falling in a band some 75 m/s wide. The exception is the large spread in velocity in the post-sunset time period.

The next four figures take the data set of Figure 4 and break it up into 10 degree wide bins of dip latitude. Figures 5 through 8 cover the ranges  $10^\circ$  to  $20^\circ$  DLAT,  $0^\circ$  to  $10^\circ$  DLAT,  $-10^\circ$  to  $0^\circ$  DLAT, and  $-20^\circ$  to  $10^\circ$  DLAT, respectively. The raw data plots indicate generally a much smaller spread in the vertical ion velocity at any given local time. The averaged plots indicate a systematic variation of the average velocity with latitude. The largest average upward velocity is

found in the most northerly latitude bin (summer hemisphere). The most southerly bin (winter hemisphere) has a net downward velocity. Other features also show latitude dependence; the evening prereversal enhancement is strong in the summer hemisphere and weak or nonexistent in the winter hemisphere.

Figures 9 and 10 show a similar pattern for the Nov 77 - Jan 78 time period. Figure 9 shows the  $10^{\circ}$  to  $20^{\circ}$  DLAT bin (winter hemisphere). Figure 10 shows the  $-20^{\circ}$  to  $-10^{\circ}$  DLAT bin (summer hemisphere). As before there is a generally upward bias of the drift in the summer hemisphere and a downward bias in the winter hemisphere.

One possible interpretation of this pattern is that the dynamo induced ion velocities are being modified by neutral wind flow, the meridional component of which flows generally from the summer to winter hemisphere under solstice conditions. Dachev and Walker, 1982, calculated the vertical ion drift velocity imposed by dynamo electric fields and the zonal and meridional winds in the 19-22 SLT range (Figure 11). These calculated patterns give good qualitative agreement with the data presented. This model also predicts longitudinal variations in the ion drift. This has not yet been tested for in the AE-E data set. Such tests should provide a useful check on this proposed mechanism. The preliminary results presented here indicate that IDM data from the AE and the more recent Dynamics Explorer B spacecraft should continue to disclose some interesting and previously unobserved dynamical features of the low-latitude F-region.

#### REFERENCES

Fejer, B. G., D. T. Farley, and C. A. Gonzales, F Region east-west drifts at Jicamarca, *J. Geophys. Res.*, 86, 215, 1981  
Dachev, T. P. and J. C. G. Walker, Seasonal dependence of the distribution of large-scale plasma depletions in the low-latitude F-region, *J. Geophys. Res.*, 87, 7625, 1982

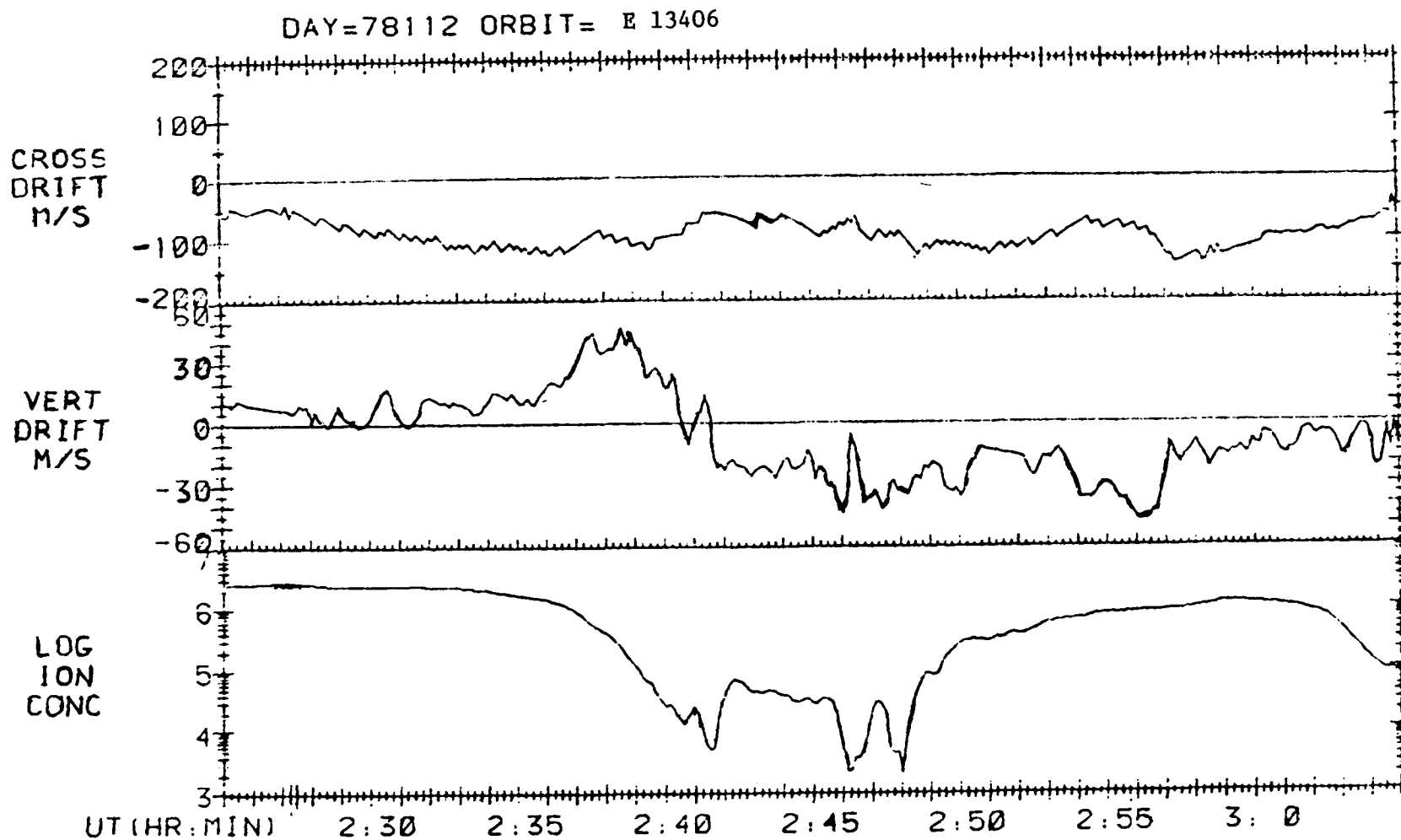


Figure 1. Data from AE-E orbit 13406 showing the sunset behavior of  $N_i$  and  $V_v$  at low dip latitudes at 315 km altitude in the Atlantic longitude sector on 22 April 1978. The post-sunset enhancement and reversal of  $V_y$  is clearly visible in this example of our routinely processed data.

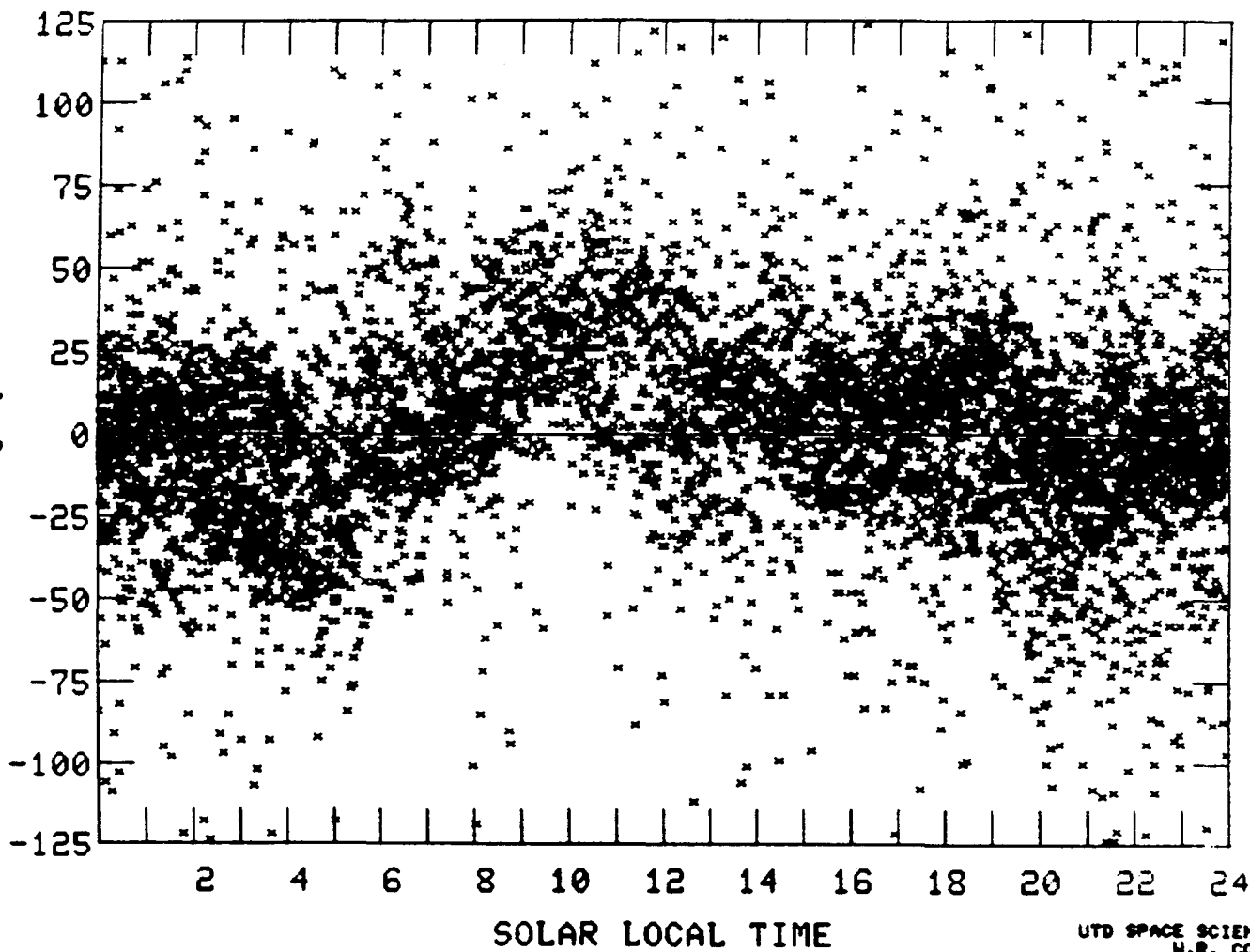
END OF TAPE REACHED  
INPUT 0 FOR AVERAGE PLOT  
INPUT 1 FOR NEW TAPE  
INPUT 2 FOR REPLOT  
WITH FLYER REJECTION:

AE-E  
78213 - 78273

ALT RANGE 800. 500.  
LAT RANGE -90. 90.  
LONG RANGE -180. 180.  
ILAT RANGE 0. 90.  
DLAT RANGE -20. 20.  
VEL RANGE -125. 125.  
MINIMUM HI 3000.

RUN NUMBER 213

32  
VERTICAL  
ION  
VELOCITY  
(M/S)



UTD SPACE SCIENCES  
W.R. COLEY

Figure 2a. Aug - Sept 1978  
-20° to 20° DLAT

HIT RETURN FOR  
RUN STATISTICS

AE-E  
78813 - 78873  
ALT RANGE 200. 500.  
LAT RANGE -90. 90.  
LONG RANGE -180. 180.  
ILAT RANGE 0. 90.  
DLAT RANGE -20. 20.  
VEL RANGE -125. 125.  
MINIMUM NI 3000.

RUN NUMBER 813

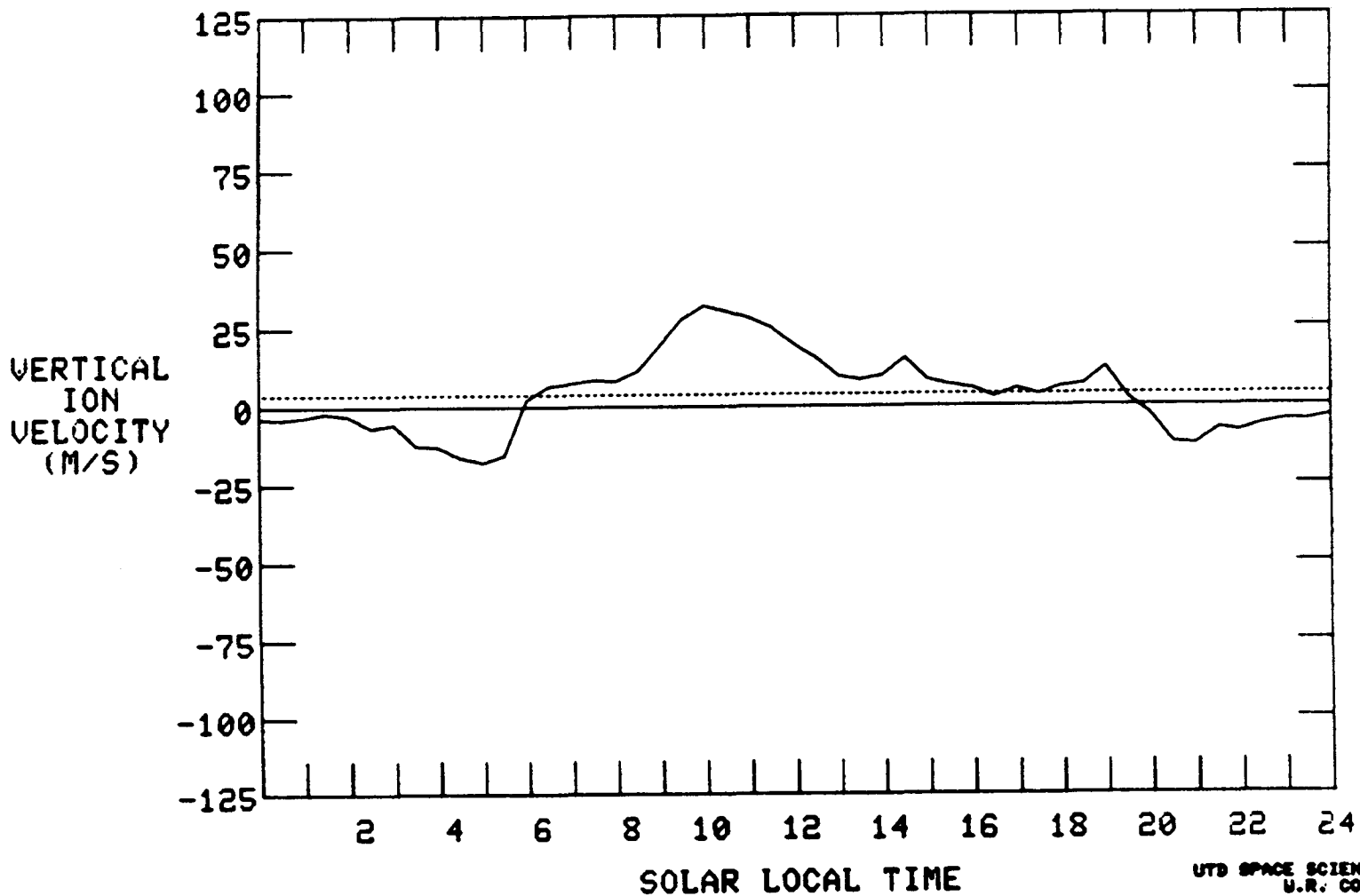


Figure 2b. Aug - Sept 1978 - 20° to 20° DLAT

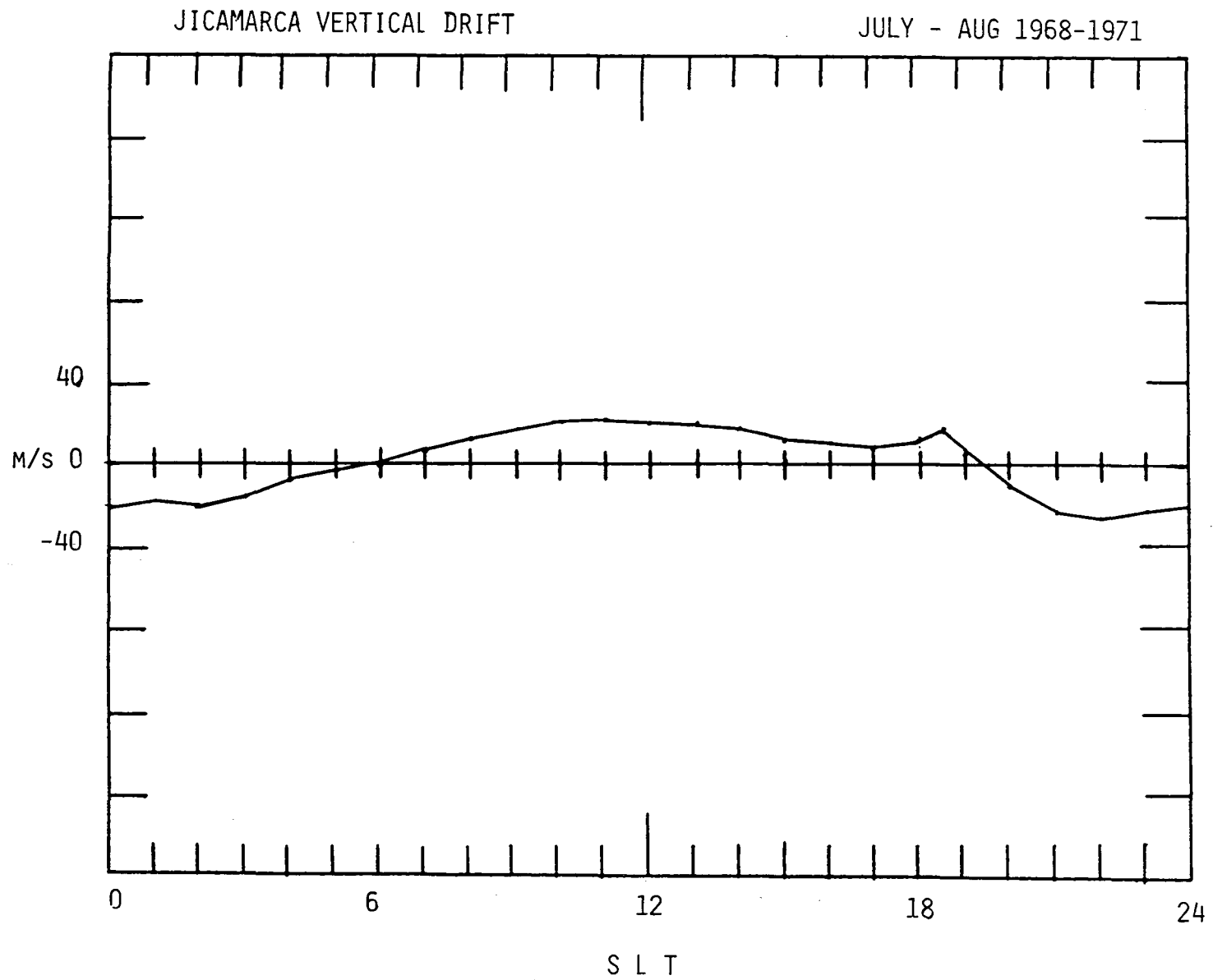


Figure 3

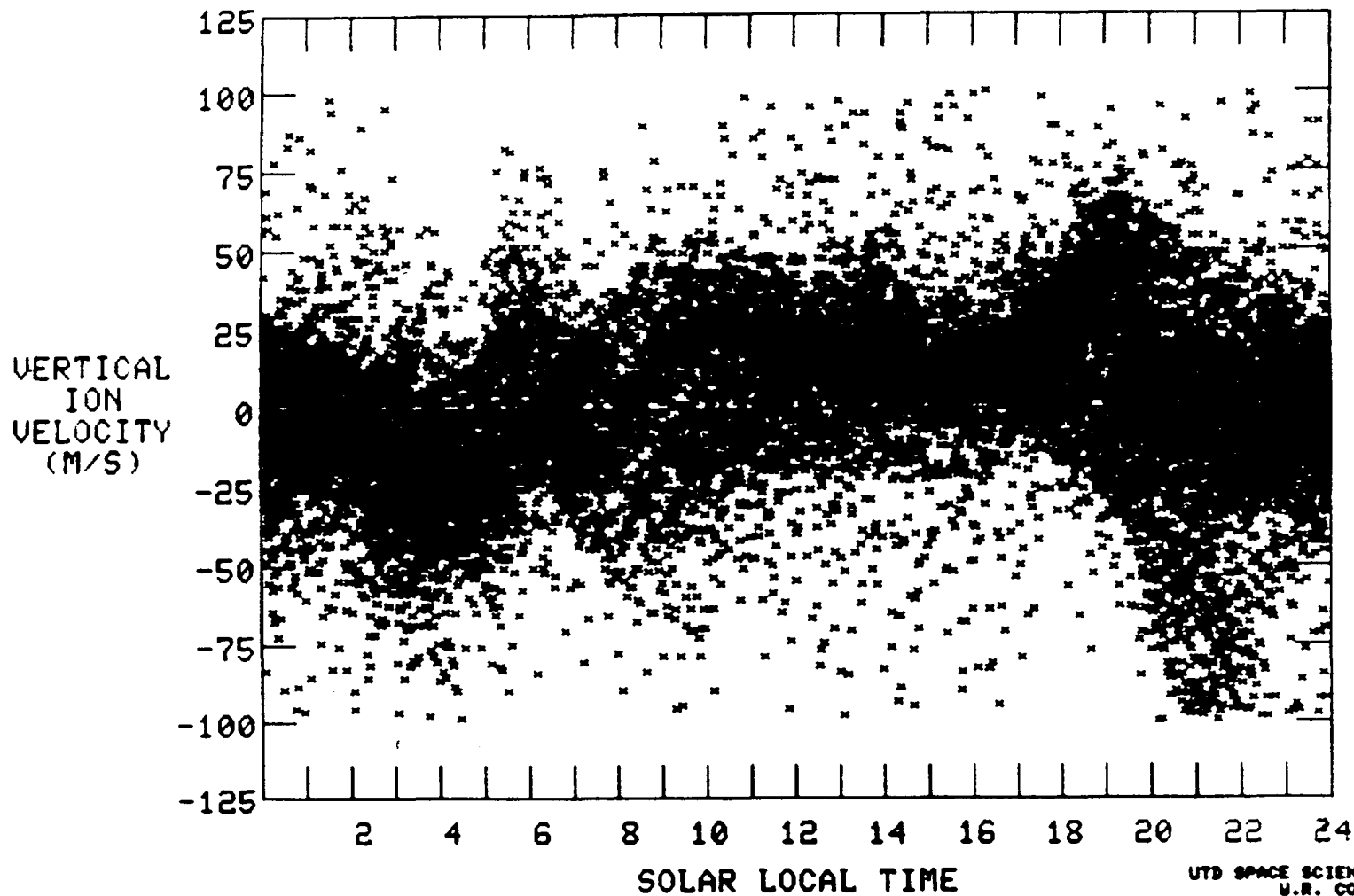
END OF TAPE REACHED  
INPUT 0 FOR AVERAGE PLOT  
INPUT 1 FOR NEW TAPE !

AE-E

79181 - 79212

ALT RANGE 200. 500.  
LAT RANGE -90. 90.  
LONG RANGE -180. 180.  
ILAT RANGE 0. 90.  
DLAT RANGE -20. 20.  
VEL RANGE -100. 100.  
MINIMUM NI 3000.

RUN NUMBER 130



UTD SPACE SCIENCES  
W.R. COLEY

Figure 4a. May - July 1979 -  $20^\circ$  to  $20^\circ$  DLAT

TTGCA -- STOP 1

PDS>

AE-E  
79121 - 79212  
ALT RANGE 200. 500.  
LAT RANGE -90. 90.  
LONG RANGE -180. 180.  
ILAT RANGE 0. 90.  
BLAT RANGE -20. 20.  
UEL RANGE -100. 100.  
MINIMUM NI 3000.

RUN NUMBER 130

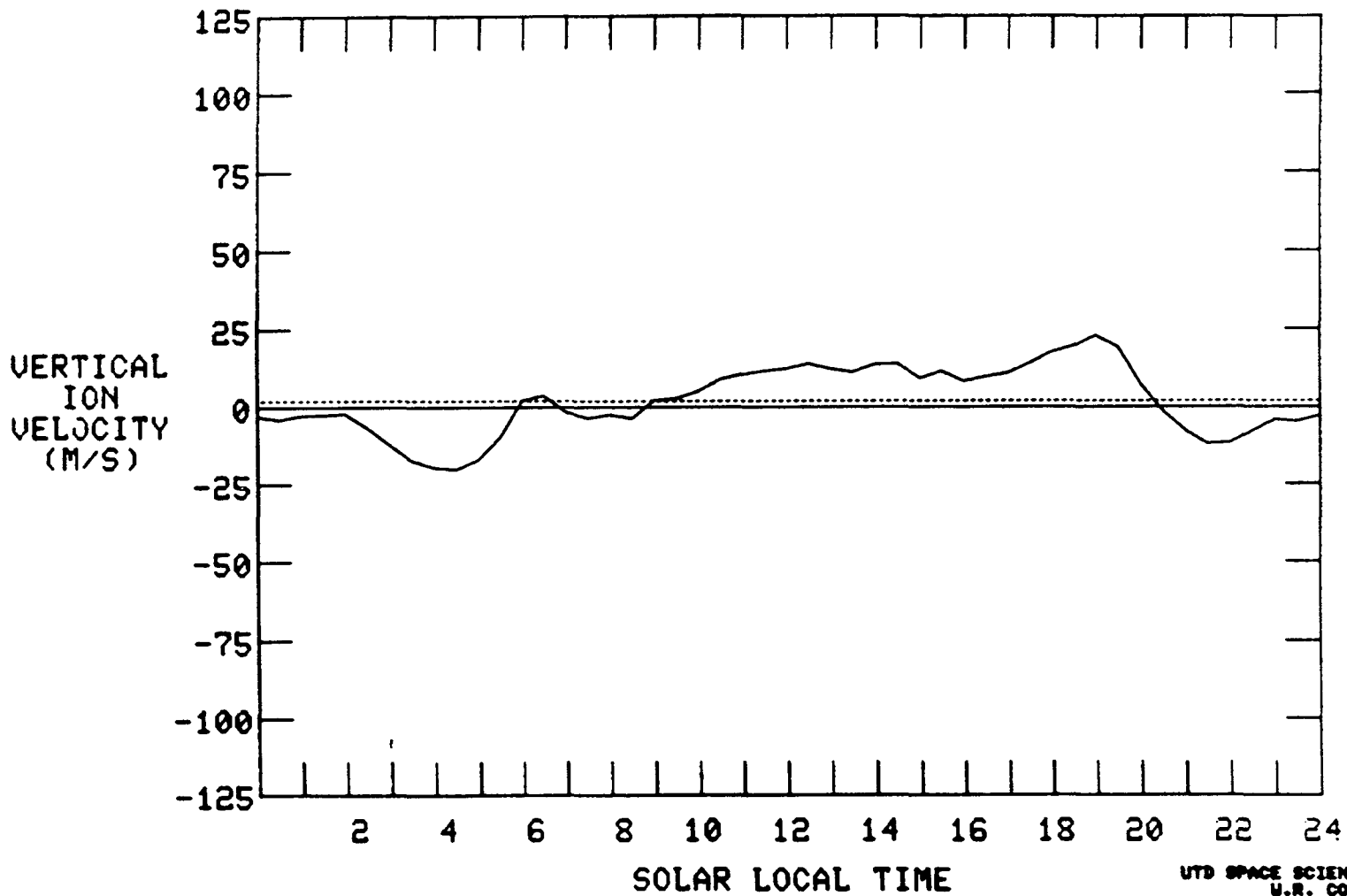


Figure 4b. May - July 1979 -  $20^\circ$  to  $20^\circ$  DLAT

END OF TAPE REACHED  
INPUT 0 FOR AVERAGE PLOT  
INPUT 1 FOR NEW TAPE :

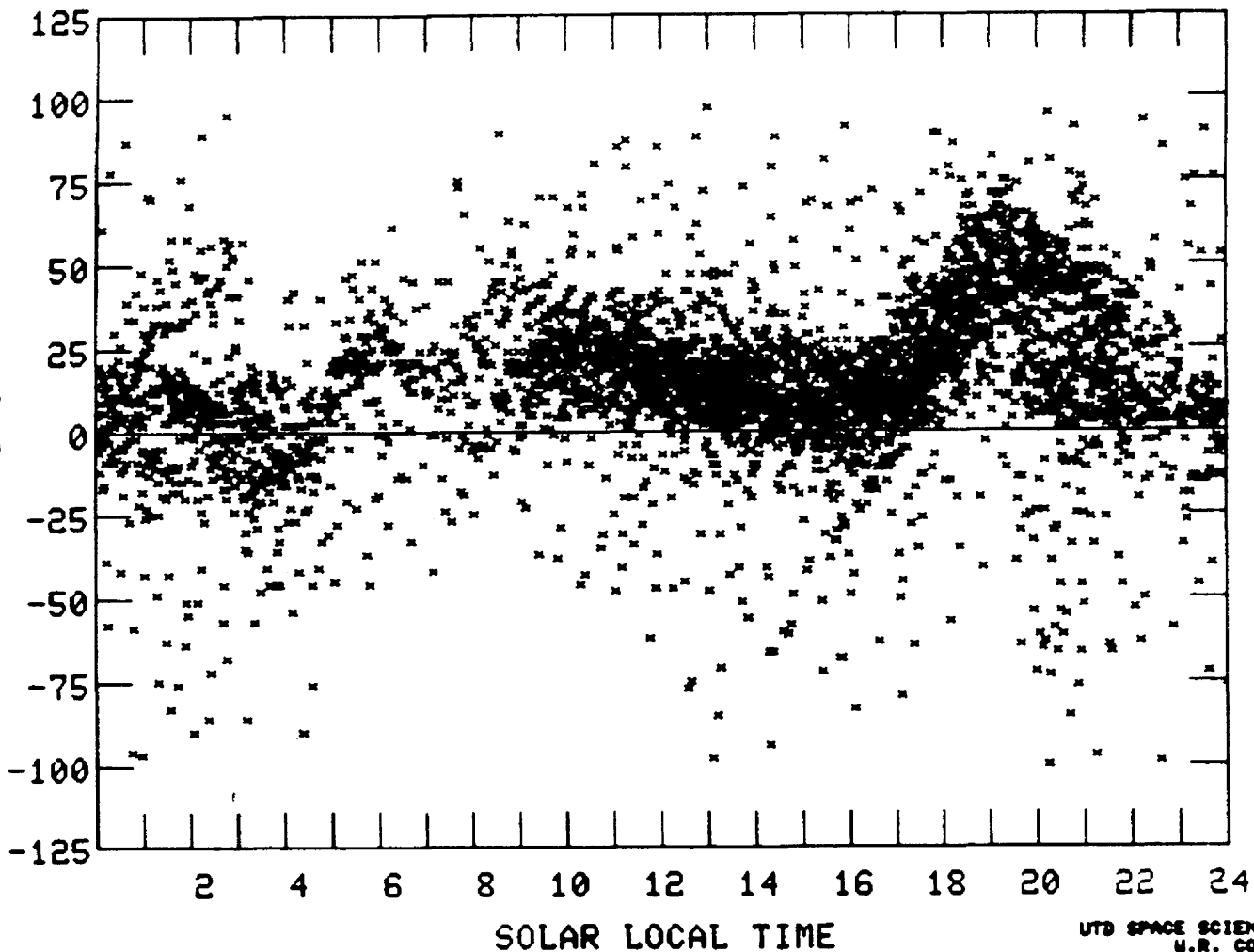
AE-E

79181 - 79212

ALT RANGE 200. 500.  
LAT RANGE -90. 90.  
LONG RANGE -180. 180.  
ILAT RANGE 0. 90.  
DLAT RANGE 10. 20.  
VEL RANGE -100. 100.  
MINIMUM HI 3000.

RUN NUMBER 136

VERTICAL  
ION  
VELOCITY  
(M/S)



UTD SPACE SCIENCES  
W.R. COLEY

Figure 5a. May - July 1979 10° to 20° DLAT

PROBA -- STOP 1

DS

AE-E  
79121 - 79212

ALT RANGE	200.	500.
LAT RANGE	-90.	90.
LONG RANGE	-180.	180.
ILAT RANGE	0.	90.
DLAT RANGE	10.	20.
UEL RANGE	-100.	100.
MINIMUM HI	3000.	

RUN NUMBER 136

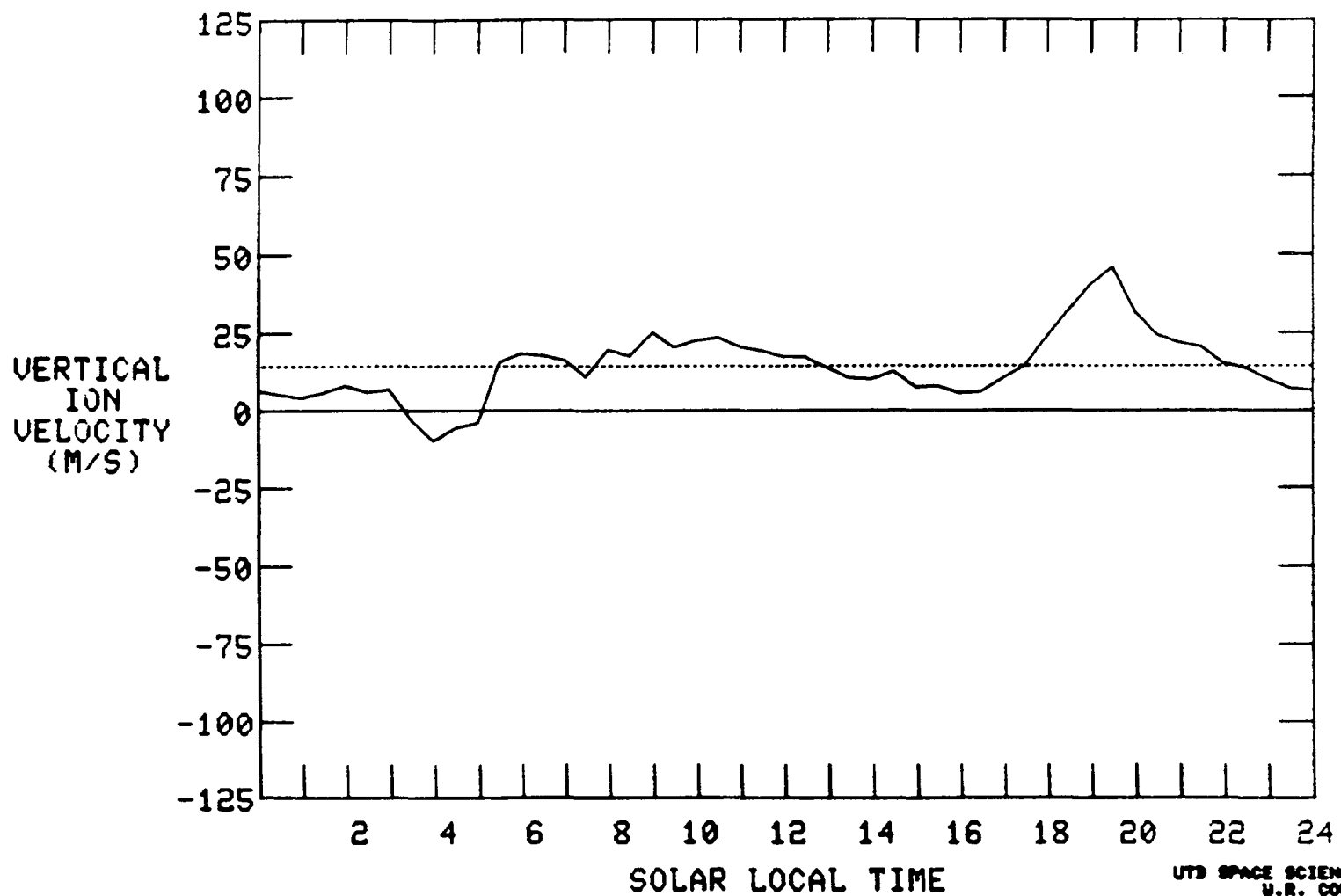


Figure 5b. May - June 1979 10° to 20° DLAT

END OF TAPE REACHED  
INPUT 0 FOR AVERAGE PLOT  
INPUT 1 FOR NEW TAPE :

AE-E  
79181 - 79218

ALT	RANGE	200.	500.
LAT	RANGE	-90.	90.
LONG	RANGE	-180.	180.
ILAT	RANGE	0.	90.
DLAT	RANGE	0.	10.
VEL	RANGE	-100.	100.
MINIMUM HI		3000.	

RUN NUMBER 136

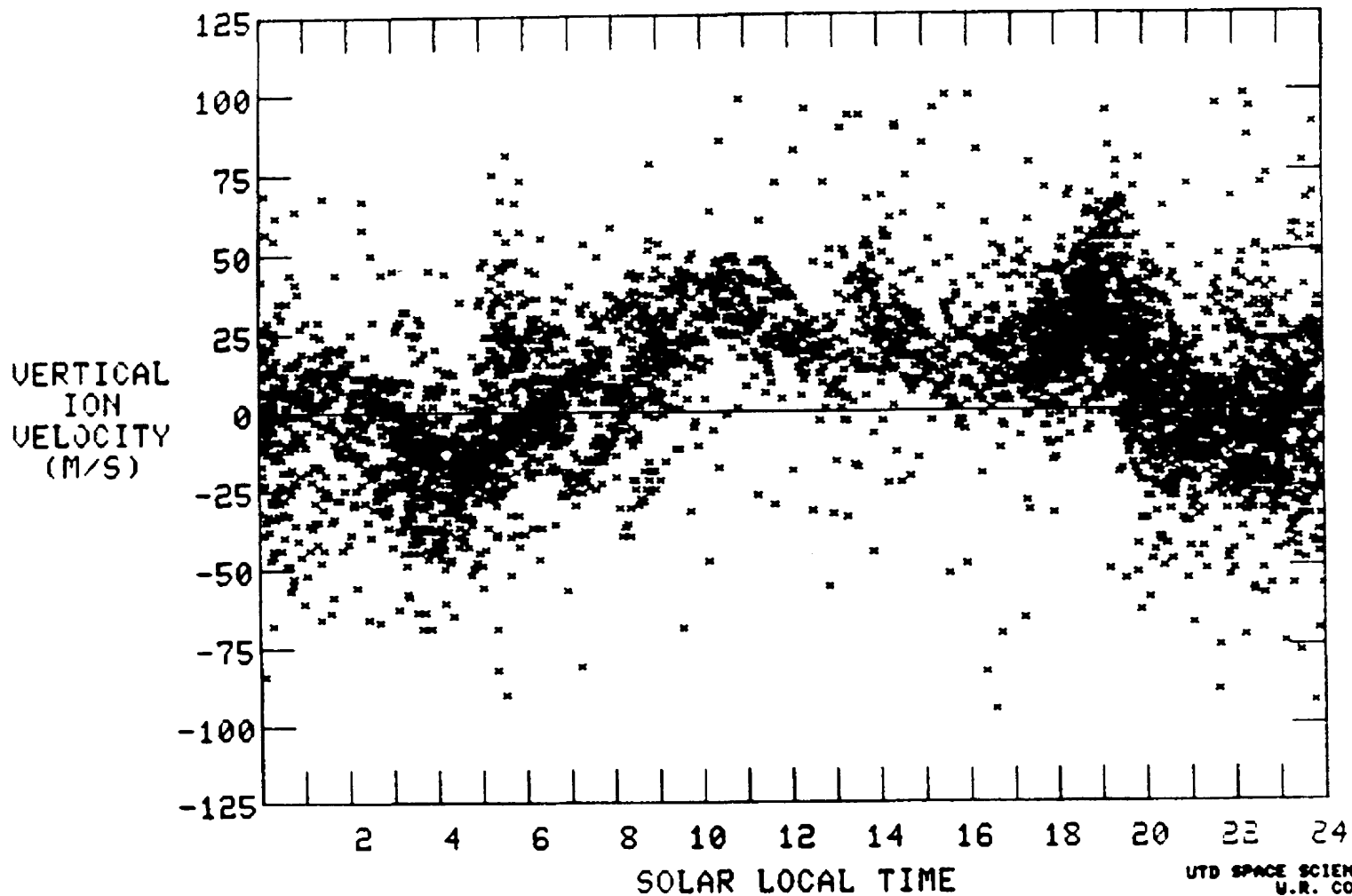


Figure 6a. May - July 1979 0° to 10° DLAT

TTOGA -- STOP 1

PDS>

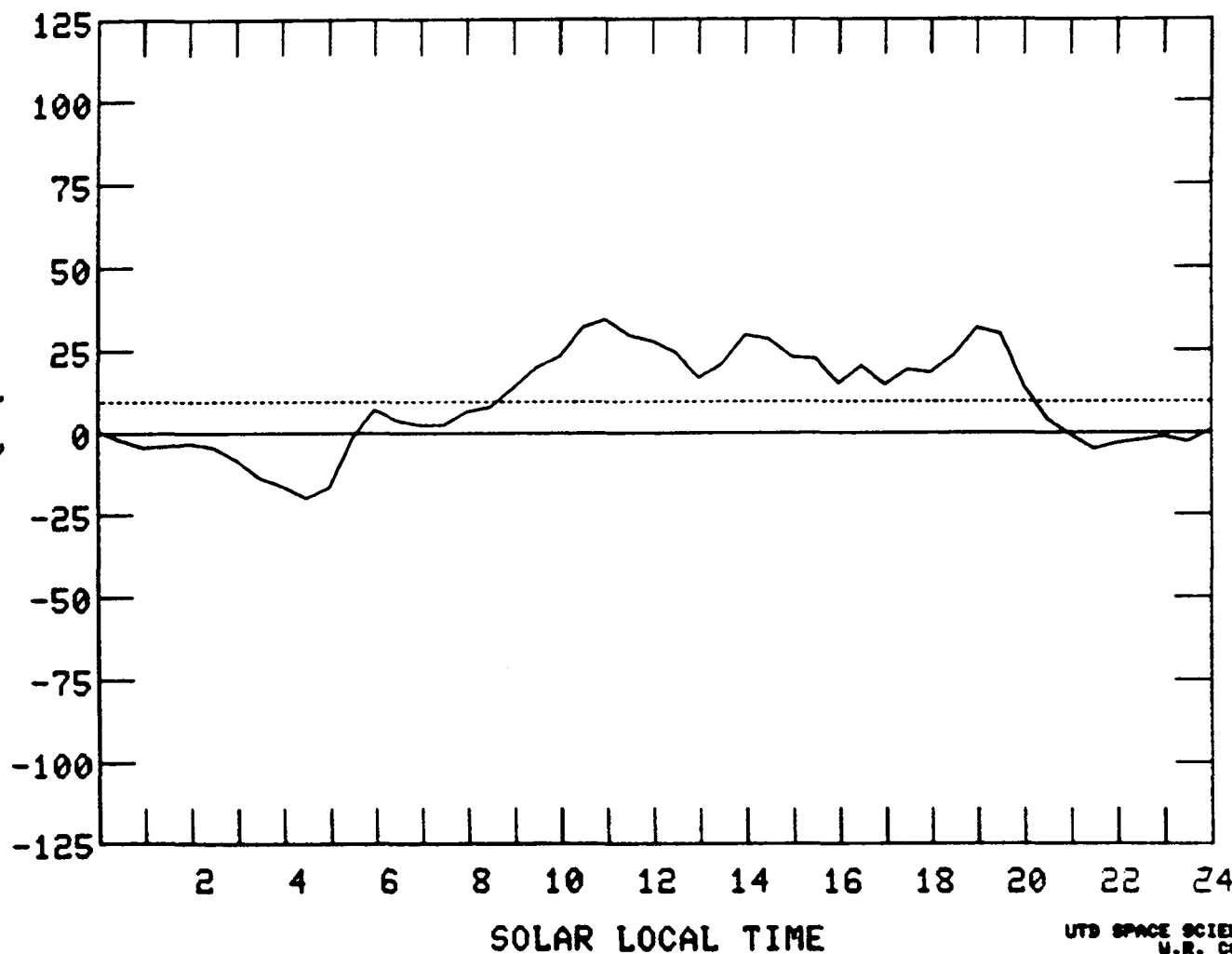
AE-E  
79121 - 79122

ALT	RANGE	200.	500.
LAT	RANGE	-90.	90.
LONG	RANGE	-180.	180.
ILAT	RANGE	0.	90.
BLAT	RANGE	0.	180.
VEL	RANGE	-100.	100.
MINIMUM NI		3000.	

RUN NUMBER 136

04

VERTICAL  
ION  
VELOCITY  
(M/S)



UTD SPACE SCIENCES  
U.R. COLEY

Figure 6b. May - July 1979 0° to 10° DLAT

END OF TAPE REACHED  
INPUT 0 FOR AVERAGE PLOT  
INPUT 1 FOR NEW TAPE ?

AE-E  
79181 - 79212  
ALT RANGE 200. 500.  
LAT RANGE -90. 90.  
LONG RANGE -180. 180.  
ILAT RANGE 0. 90.  
DLAT RANGE -10. 0.  
VEL RANGE -100. 100.  
MINIMUM NI 3000.

RUN NUMBER 137

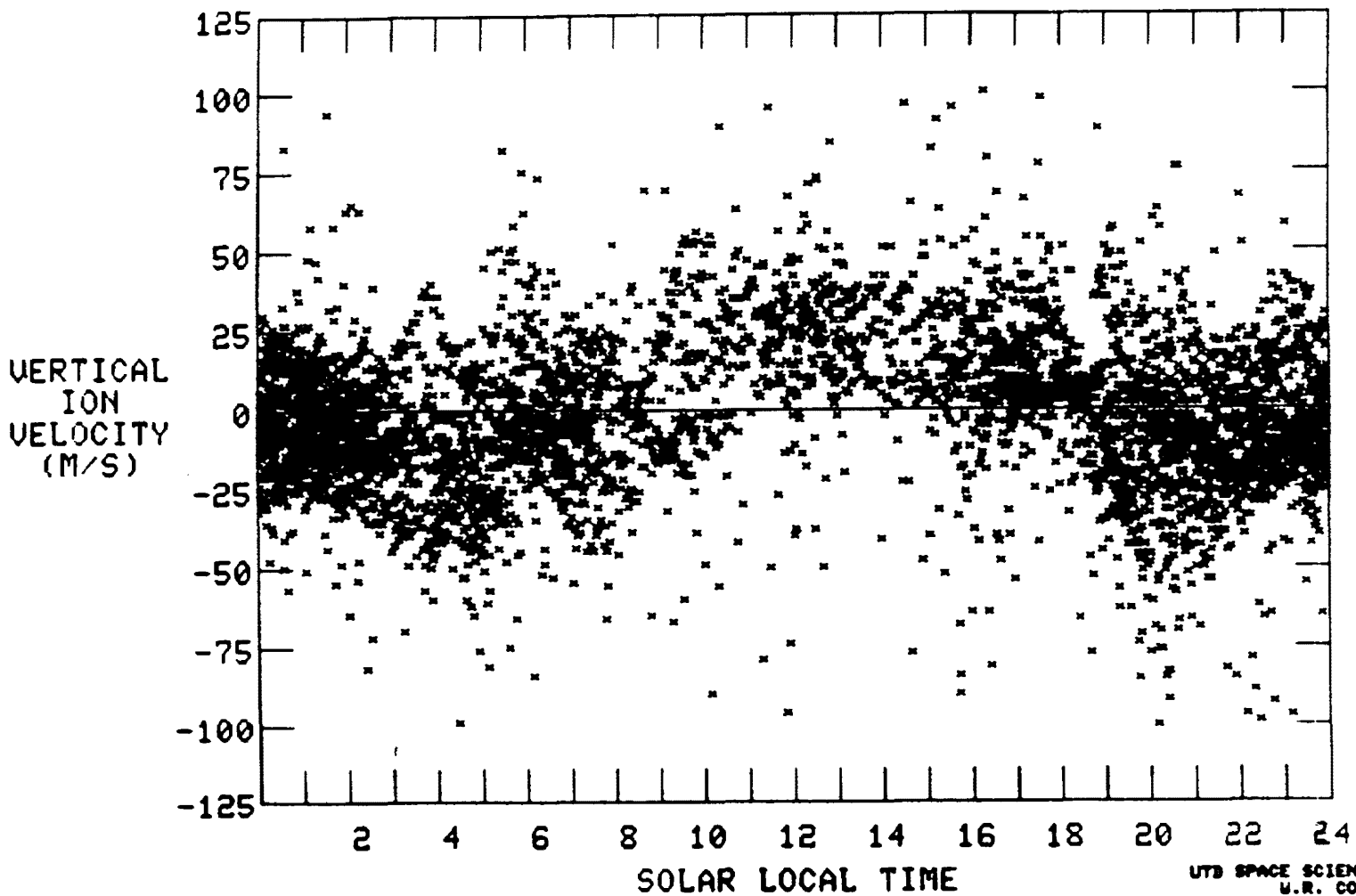


Figure 7a. May - July 1979 -  $10^\circ$  to  $0^\circ$  DLAT

TT08A -- STOP 1

NE-E  
79181 - 79818  
ALT RANGE 000. 500.  
LAT RANGE -90. 90.  
LONG RANGE -180. 180.  
ILAT RANGE 0. 90.  
DLAT RANGE -10. 10.  
VEL RANGE -100. 100.  
MINIMUM NI 3000.

RUN NUMBER 137

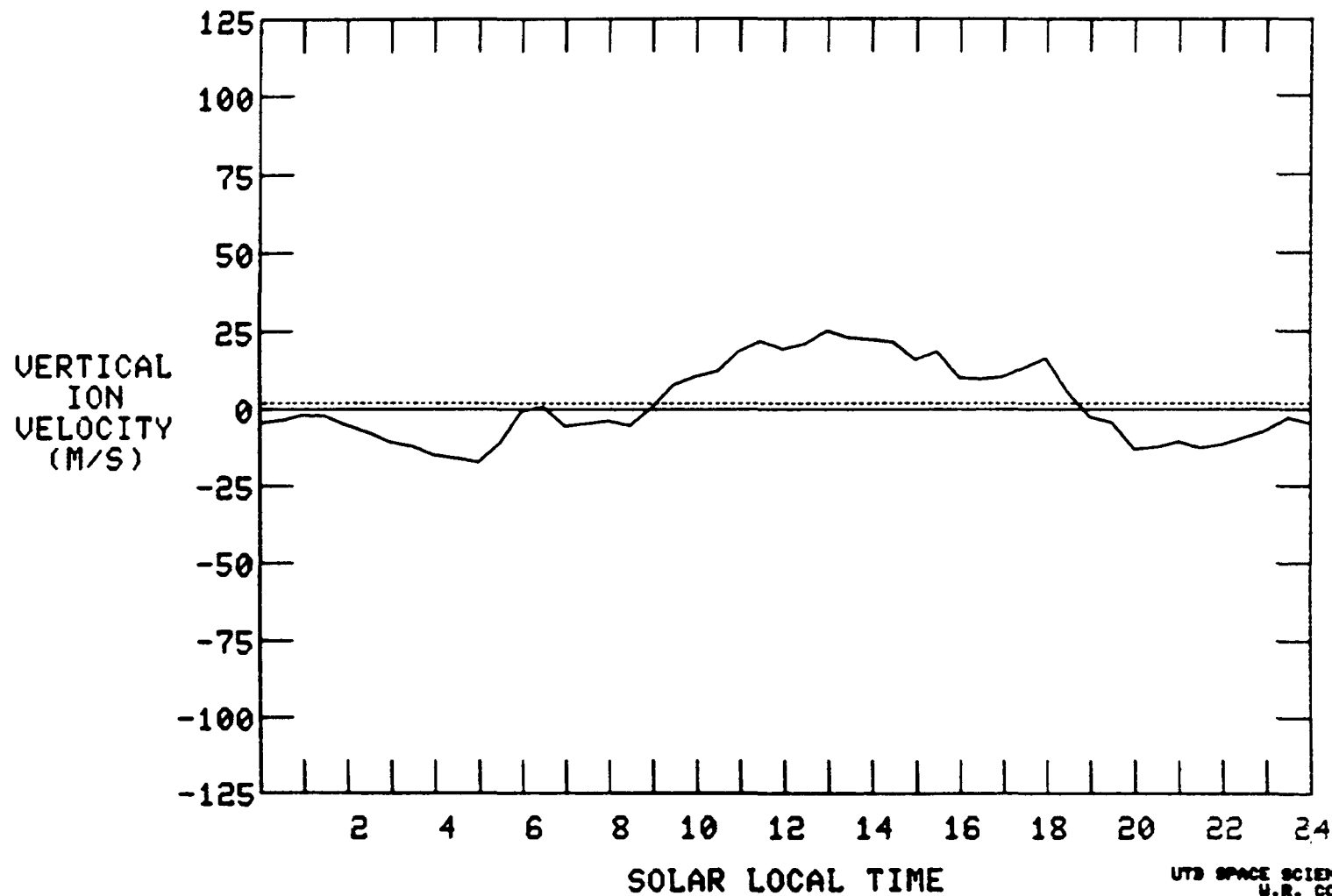


Figure 7b. May - July 1979 -  $10^\circ$  to  $0^\circ$  DLAT

END OF TAPE REACHED  
INPUT 0 FOR AVERAGE PLOT  
INPUT 1 FOR NEW TAPE !

AE-E  
79121 - 79212

ALT RANGE 200. 500.  
LAT RANGE -90. 90.  
LONG RANGE -180. 180.  
ILAT RANGE 0. 90.  
DLAT RANGE -20. 10.  
UEL RANGE -100. 100.  
MINIMUM NI 3000.

RUN NUMBER 138

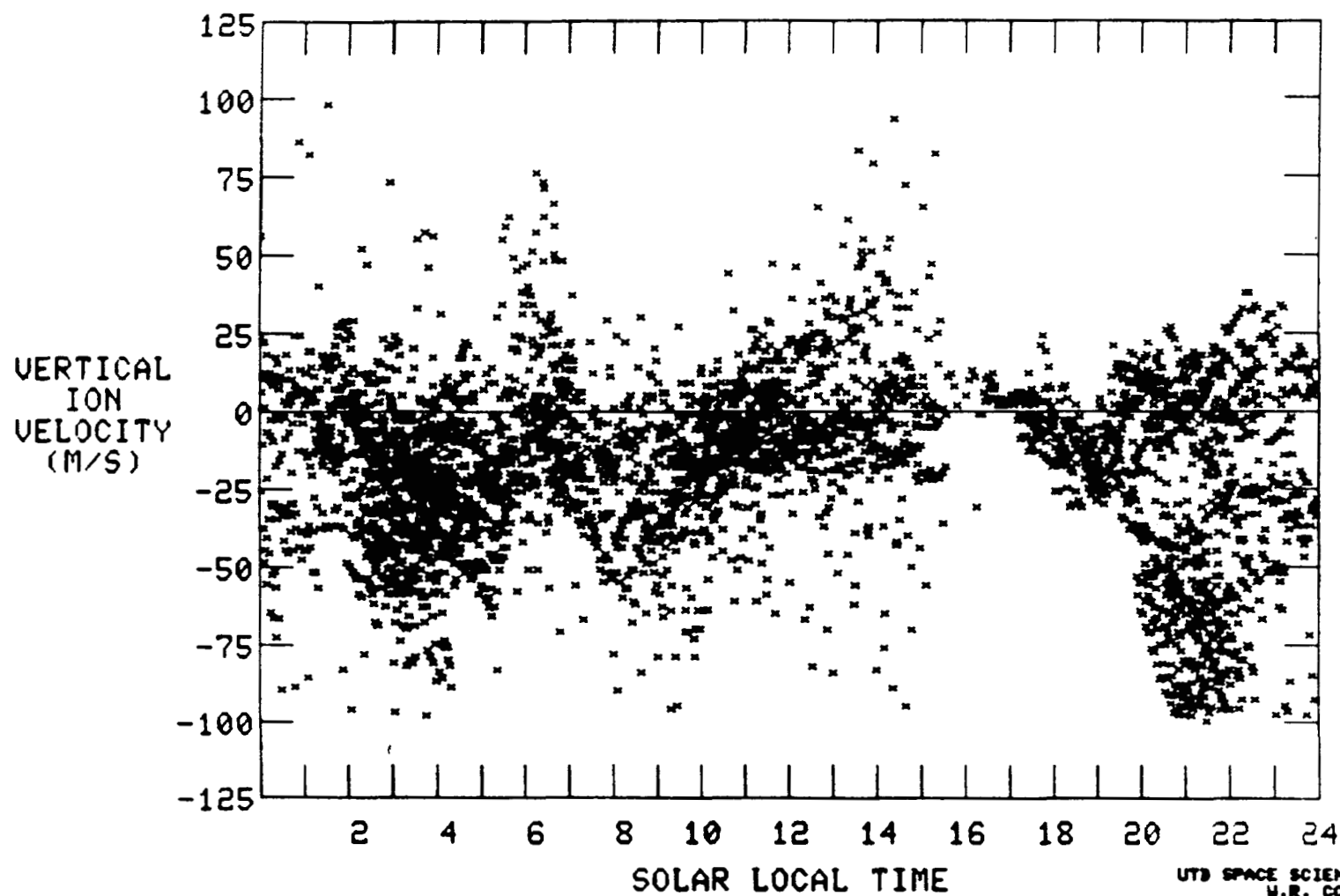
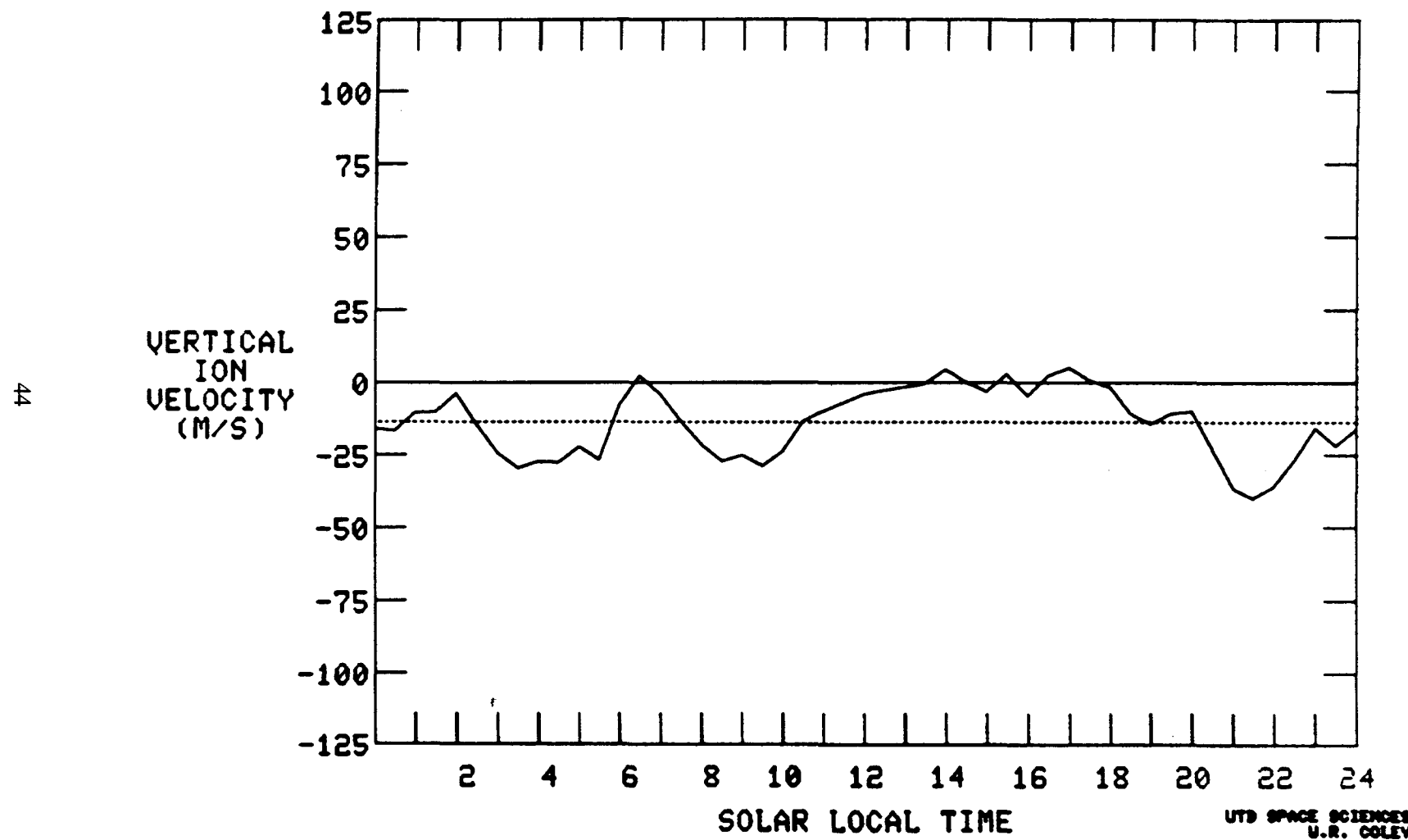


Figure 8a. May - July 1979 -  $-20^\circ$  to  $10^\circ$  DLAT

TTGSA -- STOP 1

AE-E  
79121 - 79212  
ALT RANGE 200. 500.  
LAT RANGE -90. 90.  
LONG RANGE -180. 180.  
ILAT RANGE 0. 90.  
DLAT RANGE -20. -10.  
VEL RANGE -100. 100.  
MINIMUM MI 3000.

RUN NUMBER 138



UTD SPACE SCIENCES  
U.R. COLEY

Figure 8b. May - July 1979 -  $-20^\circ$  to  $-10^\circ$  DLAT

END OF TAPE REACHED  
INPUT 0 FOR AVERAGE PLOT  
INPUT 1 FOR NEW TAPE ?

AE-E  
77365 - 78031  
ALT RANGE 200. 500.  
LAT RANGE -90. 90.  
LONG RANGE -180. 180.  
ILAT RANGE 0. 90.  
DLAT RANGE 10. 20.  
VEL RANGE -100. 100.  
MINIMUM MI 3000.

RUN NUMBER 186

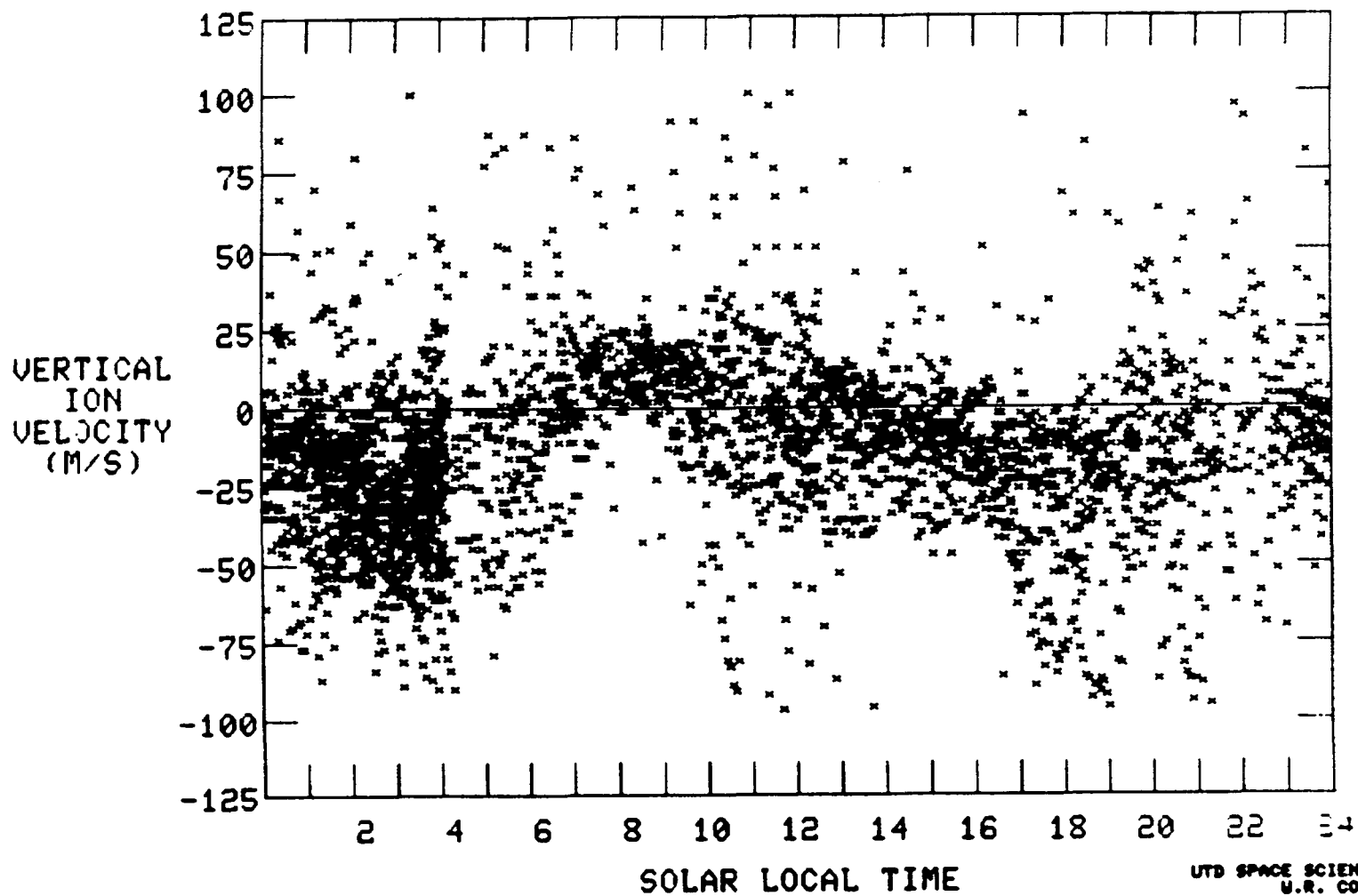


Figure 9a. Nov 1977 - Jan 1978  
10° to 20° DLAT

TT14A -- STOP 1

PDS>

AE-E  
77306 - 78031  
ALT RANGE 200. 500.  
LAT RANGE -90. 90.  
LONG RANGE -180. 180.  
ILAT RANGE 0. 90.  
DLAT RANGE 10. 20.  
VEL RANGE -100. 100.  
MINIMUM NI 3000.

RUN NUMBER 186

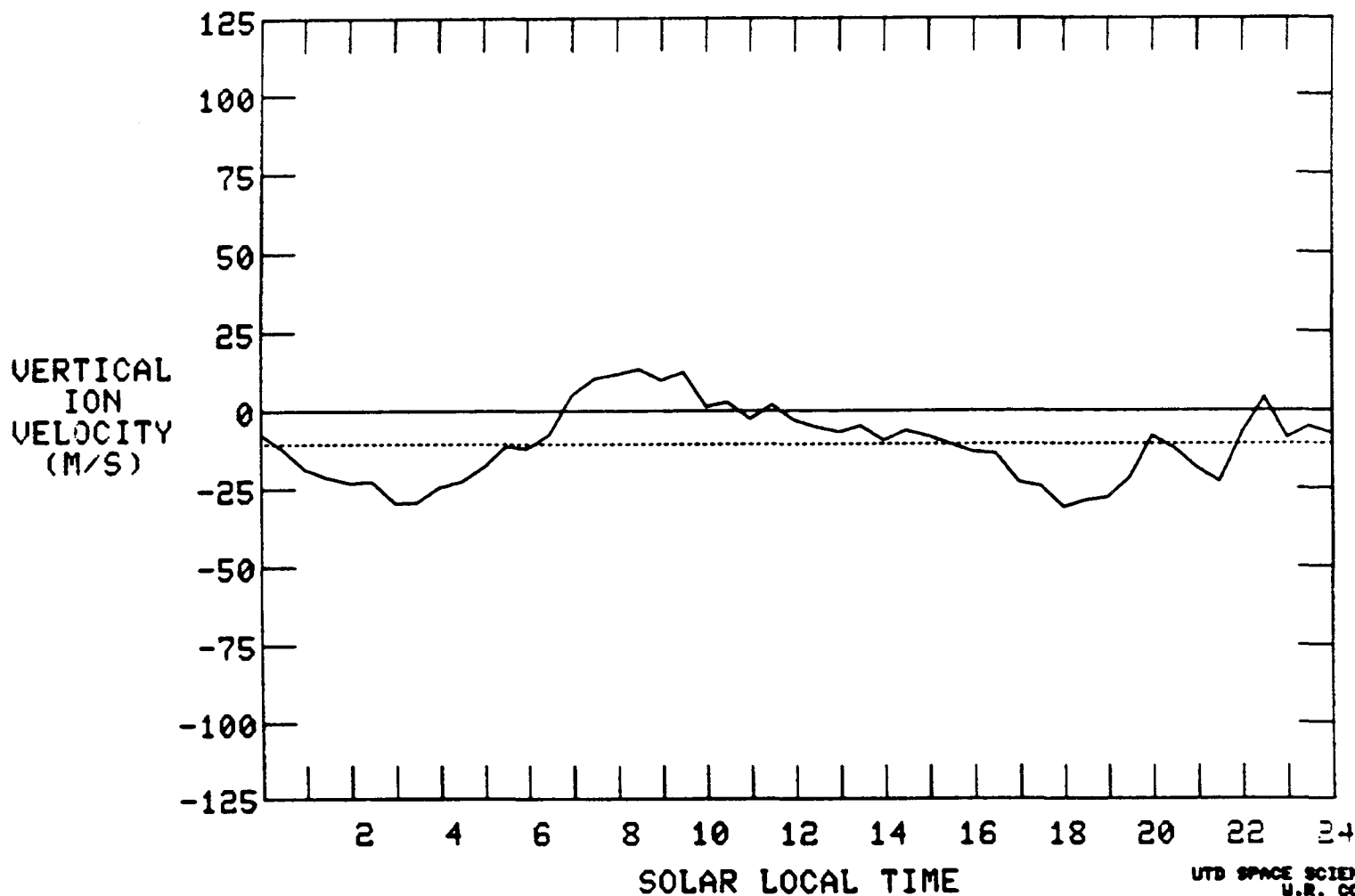


Figure 9b. Nov 1977 - Jan 1978 10° to 20° DLAT

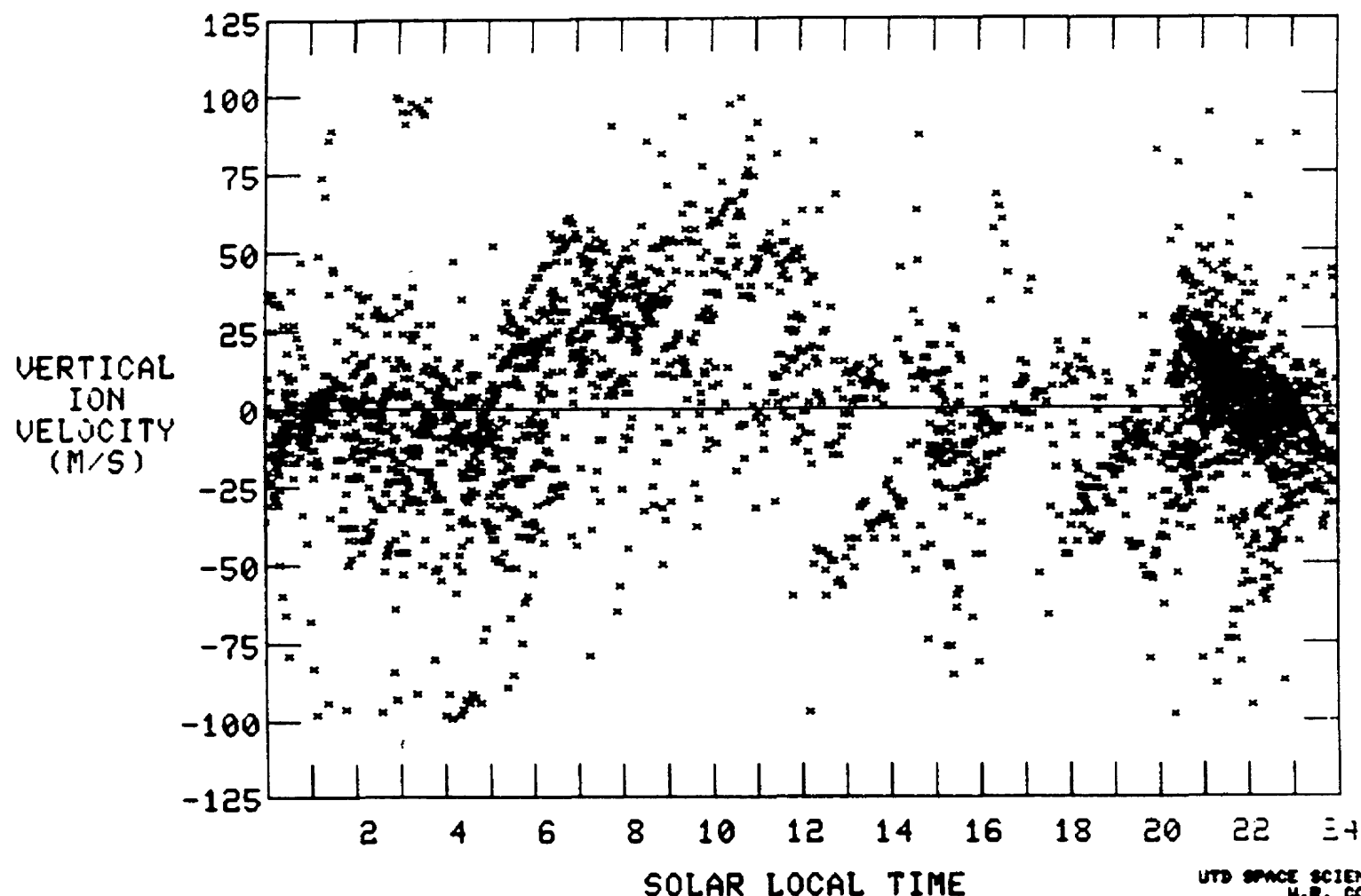
END OF TAPE REACHED  
INPUT 0 FOR AVERAGE PLOT  
INPUT 1 FOR NEW TAPE ?

AE-E

77306 - 78031

ALT RANGE 300. 500.  
LAT RANGE -90. 90.  
LONG RANGE -180. 180.  
ILAT RANGE 0. 90.  
DLAT RANGE -20. -10.  
VEL RANGE -100. 100.  
MINIMUM NI 3000.

RUN NUMBER 182



UTD SPACE SCIENCES  
W.R. COLEY

Figure 10a. Nov 1977 - Jan 1978  
-20° to -10° DLAT

TT14A -- STOP 1

PDS>

AE-E  
ALT RANGE 200. 500.  
LAT RANGE -90. 90.  
LONG RANGE -180. 180.  
ILAT RANGE 0. 90.  
DLAT RANGE -80. -10.  
VEL RANGE -100. 100.  
MINIMUM MI 3000.

RUN NUMBER 182

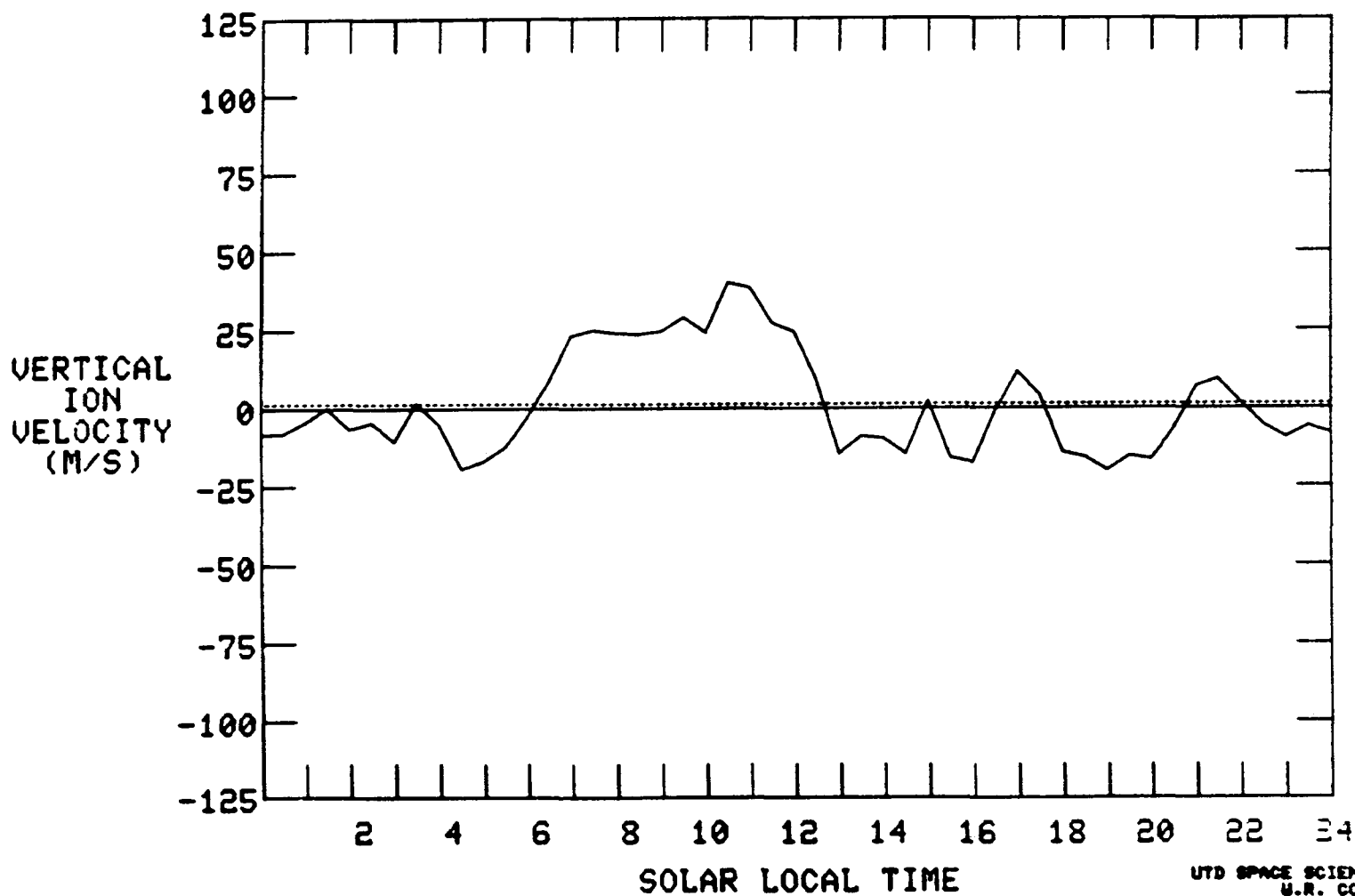


Figure 10b. Nov 1977 - Jan 1978  $-20^\circ$  to  $-10^\circ$  DLAT

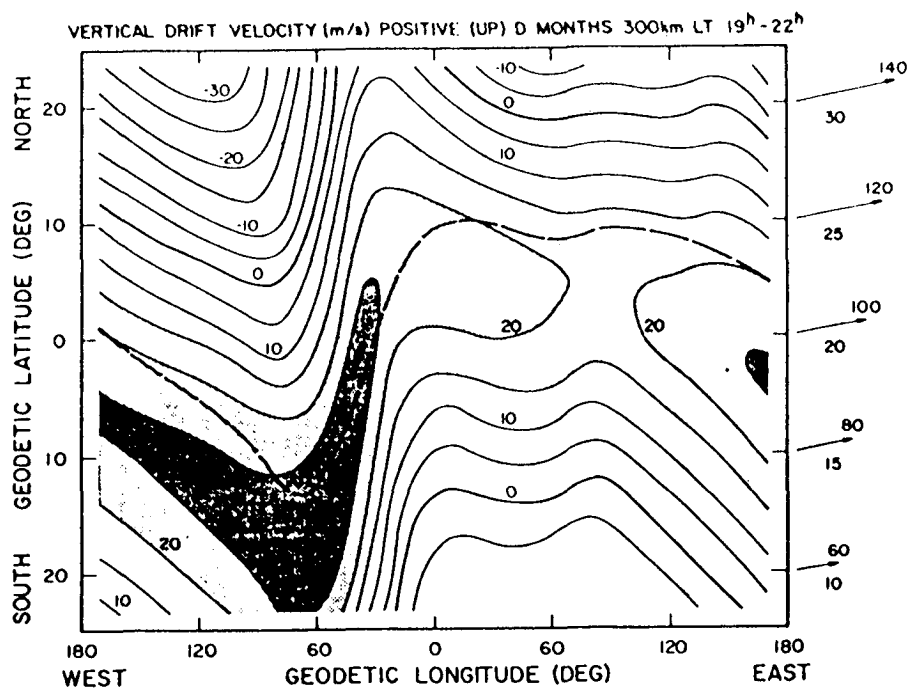


Figure 11. Contours of vertical ion drift velocity calculated for D months (northern hemisphere winter). A realistic model of the magnetic field at 300-km altitude is used for magnitude, inclination, and declination. The electric field is assumed to be constant and eastward at a value of  $0.6 \text{ mV m}^{-1}$ . The wind field varies linearly with geodetic latitude as indicated on the right-hand side of the figure. The dashed line denotes the geomagnetic equator, and the letter J refers to the Jicamarca Observatory. Regions of maximum upward drift velocity are shaded. Their locations correspond to the distribution of depleted plasma regions observed at winter solstice and shown in Figure 6.

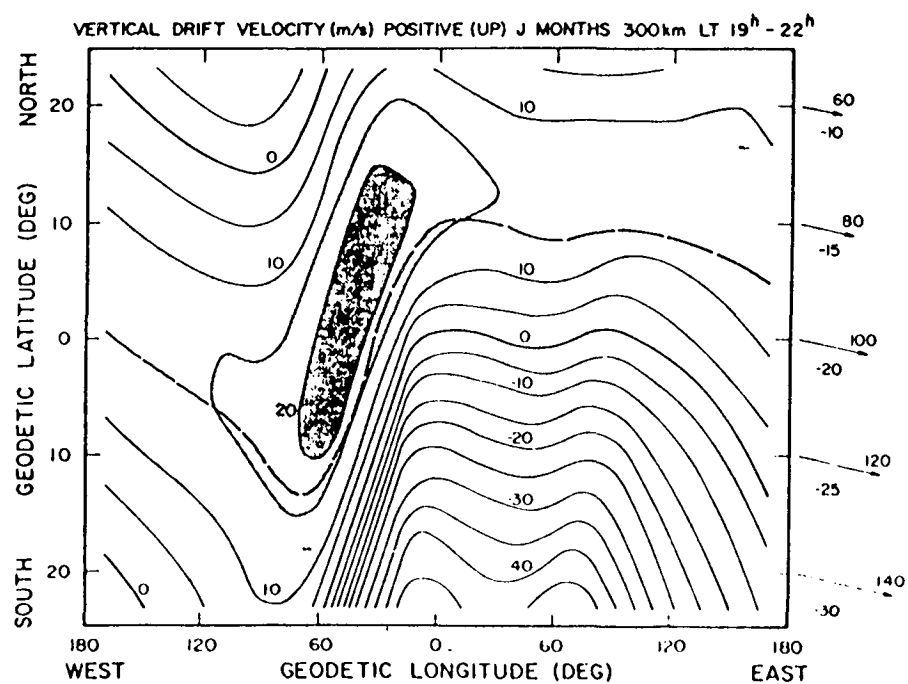


Figure 12. Vertical ion drift velocity calculated for northern hemisphere summer (J months). The wind field is the same as that used in Figure 11, with appropriate seasonal changes. Regions of maximum upward drift are shaded; their distribution corresponds closely to the observations of depleted plasma regions shown in Figure 7.